Check for updates

Probing polarity structure–function relationships in amine–water mixtures†

Elizabeth Dach, [a] Elonne Pisacane, [b] Devon Campbell, [a] Lindsay Soh [*c] and Ngai Yin Yip [*ad]

This study investigates the relationships between chemical structure, polarity, and miscibility in solvent–water systems to elucidate the mechanisms underlying the thermoresponsive hydrophilicity of amines. By integrating complementary analyses of Kamlet–Taft parameters and relative permittivity, we reveal that hydrogen bonding and nanoscale ordering, *i.e.*, molecular-level and mean-field, respectively, underlie amine–water interactions, which, in turn, influence the thermomorphic hydrophilicity.

Thermomorphic hydrophilicity solvents exhibit dramatic changes in solvent–water mutual solubilities in response to moderate changes in temperature. Raising or lowering the temperature switches the solvent between a more hydrophobic state, where the solvent is minimally miscible with water and forms a biphasic mixture, and a more hydrophilic state, where the solvent and water are completely miscible and form a single phase. A range of solvent families demonstrate thermoresponsive hydrophilicity, including ionic liquids, carboxylic acids, and epoxide-based polymers.[1–7] This study focuses on amines; water solubility in amines, especially secondary and tertiary amines, exhibits strong temperature dependence, whereas the amines have limited solubility in water, *i.e.*, solubility is directional.[2] This thermoresponsive behavior has been utilized for desalination, water softening, anti-solvent precipitation, and oil extraction.[3,6,8–10] The hydrophilic amine moieties form directional hydrogen bonds with water, facilitating water solubilization at low temperatures. As the temperature increases, the strength and prevalence of amine–water hydrogen bonds decline, resulting in phase disengagement of the amine–water mixtures into aqueous and organic phases (water- and amine-rich, respectively).[11,12] Amine–water interactions are at the heart of temperature-tunable hydrophilicity—understanding the

complex nature of mutual miscibility is critical for designing more efficient and effective solvent-driven processes and identifying novel green solvents with enhanced performance.

This study investigates the influence of solvent chemical structure, temperature, and water concentration on solvent polarity in the bulk phase and solvation shell using relative permittivity and Kamlet–Taft parameters, respectively (Fig. 1), to probe the underlying mechanisms governing the thermally toggled water affinity of thermomorphic hydrophilicity amines. Relative permittivity (ε_r) is a macroscopic measure of a solvent to screen the electric field between charges. Higher ε_r denotes greater screening, and the solvent is considered more polar. As a bulk-phase characteristic, ε_r gives information about the mean-field polarity of the solvent environment (pure amine or amine–water mixtures). The widely used Kamlet–Taft polarity scale quantifies solvent polarity by three
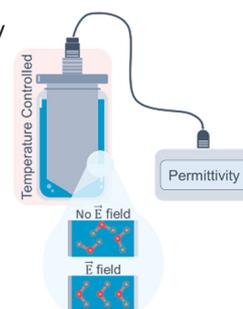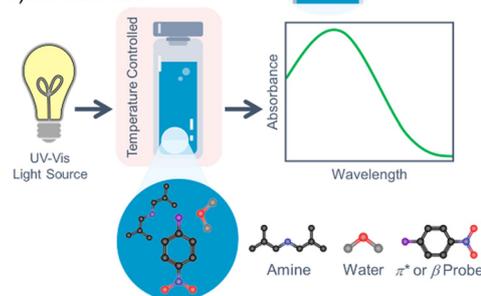
a Department of Earth and Environmental Engineering, Columbia University, New York, NY, USA. E-mail: n.y.yip@columbia.edu; Tel: +1 212 8542984
b Integrative Engineering Program, Lafayette College, Easton, PA, USA
c Department of Chemical and Biomolecular Engineering, Lafayette College, Easton, PA, USA. E-mail: sohl@lafayette.edu; Tel: +1 610 3305447
d Columbia Water Center, Columbia University, New York, NY, USA
† Electronic supplementary information (ESI) available: The supplementary information is available free of charge. See DOI: **https://doi.org/10.1039/d5cc03314d**

Fig. 1 Schematic illustrating the characterization techniques for (A) the relative permittivity, ε_r, and (B) the Kamlet–Taft polarity parameters, π^* and β.

components: hydrogen bond donor ability or acidity (α), hydrogen bond acceptor ability or basicity (β), and dipolarity/polarizability (π^*). Interactions between a chromophore-containing probe and the solvating molecules affect the position of the ultraviolet–visible spectrum absorbance band of the probe, and the frequency of maximum absorbance is utilized to determine the polarity scale parameters. Because the scale is based on interactions in the solvation shell, α, β, and π^* characterize the molecular-level polarity of the solvent system. Details of relative permittivity and Kamlet–Taft characterizations and full datasets of water- and temperature-dependent polarity scale parameters are provided in the ESI.†

Two pairs of constitutional isomeric amine solvents are investigated to isolate the effect of specific structural features on solvent polarity. Comparing dipropylamine (DPA) and diisopropylamine (DIPA) sheds light on the role of branching at the amine α-carbons, whereas juxtaposing N-ethylcyclohexylamine (ECHA) and N,N-dimethylcyclohexylamine (DMCHA) illustrates distinctions between secondary and tertiary amines (solvent structures are shown in Fig. S1, ESI†); note that, throughout this study, solvent specifically refers to the amines and not water). Each amine was evaluated with 0–7% w/w water (equivalent to approximately 0–30% mol mol^{-1}) over 25–60 °C. Observed trends across the temperature and composition ranges are analyzed against water solubility in amine to provide insights on the underlying relationship between mean-field and molecular-level solvent properties with macroscopic phase behavior. Fig. 2A shows the temperature dependence of the water mole fraction in the amine ($x_{\text{H}_2\text{O}}^{\text{amine}}$, superscript and subscript denote the solvent and solute, respectively) for DMCHA and ECHA (values reproduced from literature data).[13,14] Solubility of water in the amines decreases with increasing temperature, T. Further, $x_{\text{H}_2\text{O}}^{\text{amine}}$ is linearly correlated with T for both solvents but is more temperature-dependent for DMCHA than ECHA, decreasing by 55% and 36%, respectively, from 25 to 60 °C (equivalently, the slope of the correlation is greater in magnitude for DMCHA than ECHA, Fig. 2A). Water solubility in tertiary amines is more temperature sensitive because rotation from the additional alkyl substituent on the tertiary amine at elevated temperatures introduces greater steric hindrance around the amine nitrogen than a hydrogen atom and, hence, more markedly disrupts amine–water interactions and reduces solubility.[15,16]

Fig. 2B–D show the quantitative measures of solvent polarity for desiccated DMCHA (red square symbols, reproduced from our previous work)[17] and ECHA (yellow circle symbols). The performance of thermomorphic hydrophilicity solvents in solvent-driven water extraction is inextricably linked to interactions between the solvent and water. Thus, extrapolating information from dry solvents cannot give a complete picture of thermomorphic behavior, nor be the sole approach for identifying novel solvent candidates. However, assessing the dry solvent behavior gives insight into the components of thermoresponse that arise from innate solvent properties rather than solvent–water interactions. Here, the Kamlet Taft parameter, α, is not analyzed as the nitrogen of the secondary amines investigated in this study does not deprotonate in the environmentally relevant pH range, and the tertiary amine cannot deprotonate at the nitrogen atom. This manifests as the poor solubility of the solvatochromic probe used to determine α in the amines and the resultant unreliability of the experimental absorption measurements to
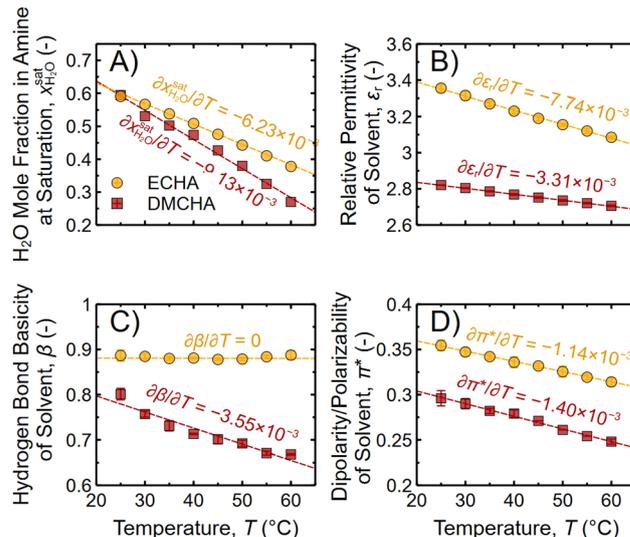

Fig. 2 Temperature-dependent properties of N-ethylcyclohexylamine, ECHA, and N,N-dimethylcyclohexylamine, DMCHA: (A) mole fraction solubility of water in amine, $x_{\text{H}_2\text{O}}^{\text{amine}}$, (B) relative permittivity, ε_r, (C) hydrogen bond acceptor ability, β, and (D) dipolarity/polarizability, π^*. Note that the amines are desiccated in (B)–(D). Data points in A are reproduced from literature,[22] whereas DMCHA data in (B)–(D) are from our previous work.[17] Data points and error bars in (B)–(D) are means and standard deviations, respectively, from duplicate samples. Dashed lines are ordinary least squares linear regressions, with slopes ($\partial/\partial T$) labeled.

determine α. Future studies may explore alternate methods for assessing hydrogen bond donation, such as ^{13}C nuclear magnetic resonance analysis.[18] Further, because of the basicity of the amines, water is expected to be the dominant hydrogen bond donor in amine–water mixtures. This is substantiated by $\beta = 0.19$ and 0.74–0.90 for water and the amines, respectively, at 25 °C. Therefore, hydrogen bonding behavior in mixtures, discussed later, is captured by β characterization of the amines.

Temperature-driven changes in the molecular-level polarity (Fig. 2C and D), representative of cybotactic solvent molecules interacting with water, reflect the observed decline in amine–water miscibility at elevated temperatures (Fig. 2A). Both π^* and β decrease as temperature increases, and the parameters are more temperature-sensitive for DMCHA than ECHA. These trends support the explanation that increased steric hindrance on the amine nitrogen of tertiary amines over secondary amines decreases overall hydrogen bonding (β of DMCHA < ECHA across the range of T investigated) and increases the thermoresponsiveness of hydrogen bond acceptance, as evidenced by $\partial\beta/\partial T$ being significantly larger for DMCHA than ECHA. π^* of DMCHA is lower than ECHA across the range of T investigated, reflecting the lower dipole moment of DMCHA (0.76 vs. 1.46). The temperature dependence of dipolarity/polarizability is only marginally larger for DMCHA than ECHA, indicating that, while both π^* and β contribute to the greater thermoresponsiveness of DMCHA–water miscibility, changes in hydrogen bonding are the dominant factor.

Conversely, relative permittivity (ε_r, Fig. 2B), which describes the mean-field polarity, does not parallel the temperature dependence of $x_{\text{H}_2\text{O}}^{\text{amine}}$. Although ε_r decreases with increasing temperature for both solvents, ε_r of ECHA changes more with temperature than DMCHA, opposite to the miscibility trend shown in Fig. 2A. These results

highlight that water solubility in amines is principally governed by molecular-level interactions between solvent–solvent and solvent–water and that important features of temperature sensitivity will be overlooked if the solvent is approximated as a dielectric continuum.

For the branched-linear isomer comparison between DIPA and DPA, however, none of the polarity parameters reflect the elevated temperature sensitivity of $x_{H_2O}^{amine}$ for DIPA compared to DPA (Fig. S2 of the ESI†). DIPA is fully miscible with water at 25 °C and passes through a lower critical solution temperature (LCST) at 28 °C.[14] Above its LCST, water solubility in DIPA continues to be more temperature-dependent than in DPA (51% and 21% decrease from 30 to 60 °C, respectively). However, ε_r, π^*, and β are all more temperature-dependent in DPA (i.e., higher $\partial/\partial T$). Branching on the amine α-carbons in DIPA decreases overall hydrogen bonding (lower β than DPA for the range of T investigated) but does not increase the thermoresponsiveness of hydrogen bond acceptance, in contrast to the observed trends in the earlier secondary-tertiary amine analysis. The ε_r, π^*, and β characterizations are carried out on desiccated pure solvents, i.e., water is absent. Thus, the pronounced temperature-sensitivity of $x_{H_2O}^{amine}$ for DIPA compared to DPA must arise from phenomena that occur only in amine–water mixtures rather than from inherent properties of the dry solvent. The dry solvent analysis captures nuanced distinctions in DIPA and DPA self-association, i.e., amine–amine interactions, but the magnitude of amine–amine interactions is minor relative to amine–water interactions in mixtures.[12] Thus, we posit that the contrast between tertiary DMCHA and secondary ECHA is large enough that the

disparities in polarity between desiccated pure solvents are reflective of differences in amine–water mixtures; conversely, the subtle variations between DIPA and DPA, two secondary amines, are overwhelmed by divergences in amine–water interactions.

As water is introduced into the amines within the monophasic region of the systems, ε_r expectedly increases toward the value of pure water (78.3 at 25 °C and 66.8 at 60 °C),[19] as presented in Fig. 3. If the amine–water mixtures are ideal, ε_r should increase linearly as a volume fraction (ϕ) weighted average of the relative permittivities of the pure amine and water $(\varepsilon_r^{mix,ideal} = \phi_{amine}\varepsilon_r^{amine} + \phi_{H_2O}\varepsilon_r^{H_2O})$,[20] shown as dot-dashed lines in Fig. 3. ε_r of the amine–water mixtures consistently falls below the ideal ϕ-weighted average. Associations between the amine and water molecules (i.e., hydrogen bonding and van der Waals interactions) cause negative deviations from ideal mixing.[21,22] The magnitude of the deviation from the ideal mixture is indicative of the strength and prevalence of heteromolecular interactions (i.e., amine–water and not water–water or amine–amine). We note that there are inherent limitations to linear dielectric mixing models, which assume homogeneous solutions, i.e., no microstructuring or inhomogeneities at mixture interfaces, and do not account for potential volume contraction/expansion due to species interactions. Nevertheless, comparing the relative deviation from ideal linear mixing of different amine–water mixtures yields pertinent insights into the water- and temperature-sensitivity of the systems.

For DPA and ECHA, the experimental ε_r decreases monotonically with increasing T across all ϕ_{H_2O} investigated (red symbols are lower than blue symbols at each water content in Fig. 3B and D). A more complex picture emerges for DIPA and DMCHA (Fig. 3A and C): while the inverse influence of T on ε_r is valid at lower ϕ_{H_2O}, the trend does not hold at higher ϕ_{H_2O}, with ε_r first dropping and then rising with higher temperatures. This is alternatively represented by ε_r tending upward, toward $\varepsilon_r^{mix,ideal}$, at elevated temperatures and water contents. The solid red lines in Fig. 3A and C illustrate this behavior at 60 °C for DIPA and 50 °C for DMCHA, resulting in crossing the solid blue lines (for DMCHA, mixtures above 50 °C phase separate at ϕ_{H_2O} = 0.06 and, hence, higher T is not evaluated). The diminishing deviation of experimental ε_r from an ideal mixture provides evidence that, compared to DPA and ECHA, DIPA- and DMCHA–water mixtures show reduced amine–water interactions and greater water–water and amine–amine interactions, i.e., the molecules begin to self-associate. Small-angle X-ray scattering studies have observed nanoscale water clustering in water–DIPA mixtures.[12] We posit that the onset of water aggregation is associated with the trend toward more homomolecular interactions. Further studies can elucidate the temperature dependence of these aggregates and probe the universality of the homoaggregation across other amine–water mixtures, possibly at higher ϕ_{H_2O} and T. Hetero- or homomolecular association and the resultant aggregation occur at longer length scales than directional solvent–solvent or solvent–water interactions, so relative permittivity is better suited to probe this phenomenon than Kamlet–Taft analysis, which is limited to the solvation shell around the chromophoric dye. Integrating these complementary tools enables a more complete understanding of the system to reveal that the molecular configuration of the water-laden solvent is a crucial contributor to the increased temperature sensitivity of branched DIPA over linear DPA and tertiary DMCHA over secondary ECHA.
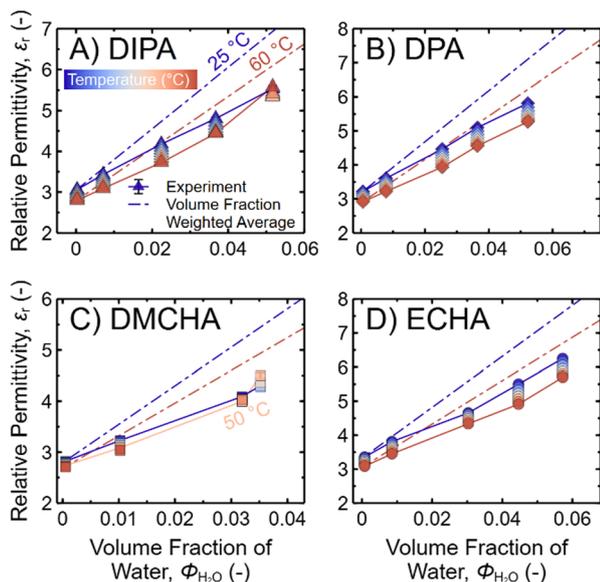

Fig. 3 Relative permittivity, ε_r, as a function of water volume fraction, ϕ_{H_2O}, in the amine–water monophasic mixtures for (A) diisopropylamine (DIPA), (B) dipropylamine (DPA), (C) N,N-dimethylcyclohexylamine (DMCHA), and (D) N-ethylcyclohexylamine (ECHA). Data points and error bars are means and standard deviations, respectively, for duplicate samples. Note that due to the high reproducibility of the measurement technique, most error bars are smaller than the symbols. Solid lines connect experimental data points, and dot-dashed lines model ε_r as a ϕ-weighted average. Color of the symbols and lines denotes the temperature from 25 °C to 60 °C (dark blue and dark red, respectively).

Hydrogen bond basicity, *i.e.*, H-bond acceptor ability, can shed light on additional synergistic effects in amine–water mixtures. Pure water is a weaker hydrogen bond acceptor than any of the investigated amines, with $\beta_{H_2O} = 0.19$ compared to $\beta = 0.74$–0.90 for the amines at 25 °C. However, as water is introduced to the amines, β_{mix} increases and is higher than β of the pure amine (Table S2 of the ESI†). Unlike ε_r and π^* (Tables S1 and S3, respectively, ESI†), which trend toward the pure water values as ϕ_{H_2O} increases, amine–water mixtures are better hydrogen bond acceptors than either pure component. The excess β values (β^E), defined as $\beta^E = \beta_{mix} - (\phi_{amine}\beta_{amine} + \phi_{H_2O}\beta_{H_2O})$, as a function of water volume fraction in the mixtures (ϕ_{H_2O}) are shown in Fig. 4. This synergism suggests the formation of amine–water complexes, which are better hydrogen bond acceptors than either pure solvent.[23–25] These complexes may form domains or interfaces that can preferentially interact with the solvatochromic probe used to determine β. Accounting for this synergistic effect and the earlier homoaggregation will yield more accurate thermodynamic models of amine–water systems. Water partitioning into amines is enthalpically driven, particularly by amine–water hydrogen bonding.[26] Incorporating the elevated hydrogen bond acceptor ability of amine–water mixtures and the nanoscale ordering of H_2O molecules will shift the balance between enthalpically favorable amine–water interactions and entropically unfavorable water structuring in the organic phase. The drop in the experimentally characterized β^E at high ϕ_{H_2O} may be due to the selective solvation of the Kamlet–Taft probe molecule by water over amine, and additional studies are needed to further elucidate the reversion of β^E to zero.

Thermomorphic hydrophilicity solvents have shown promise to be an emerging platform for novel chemical separations and water purification technologies. The working principles of these innovations are based on the reversible thermal response of the solvent properties, with prior studies showing that amines can be cycled repeatedly between low and high temperatures (*i.e.*, between more hydrophilic and hydrophobic states) while maintaining separation performance.[3] This study showed that integrating molecular-level and mean-field polarity analyses can shed light on the structure–property–performance relationship of thermoresponsive amine–water systems. In particular, the findings highlight the importance of branching near the amine nitrogen to increase the temperature dependence of amine–water association; the relative permittivity analysis suggests that amine and water self-association are key drivers of the thermal response. Further understanding the fundamental mechanisms governing the thermomorphic response will be critical in the design and discovery of novel green solvents with enhanced performance. To further build upon the information gleaned on the solvation shell and mean field polarity of amines and amine–water mixtures, investigations into intermediate length scales, *e.g.*, using small-angle X-ray scattering or dynamic light scattering techniques, are a fruitful area for additional research. The non-ideal dielectric behavior observed in amine–water mixtures can be further elucidated through deeper analysis, *e.g.*, examination of the Kirkwood correlation factor. The insights gained into amine–water mixtures will also advance the understanding of other organic–aqueous biphasic mixtures that exhibit lower critical solution temperatures, where enthalpically-favorable hydrogen bonding in competition with entropically-unfavorable molecular ordering determines mixing behavior.
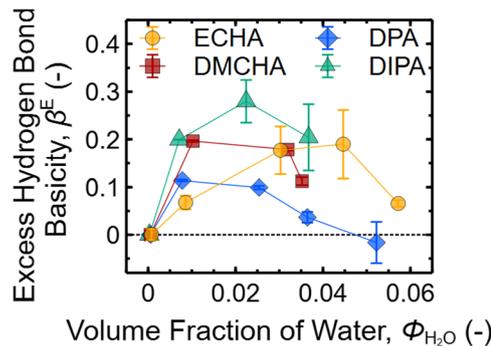

Fig. 4 Deviation of hydrogen bond basicity (β^E) from the volume fraction (ϕ_{H_2O})-weighted average as a function of ϕ_{H_2O} in the amine–water system at 25 °C for diisopropylamine (DIPA), dipropylamine (DPA), *N,N*-dimethylcyclohexylamine (DMCHA), and *N*-ethylcyclohexylamine (ECHA). Data points and error bars are means and standard deviations, respectively, for duplicate samples.

Conflicts of interest

The authors declare no conflicts of interest.

Data availability

The data supporting this article have been included as part of the ESI.†

Notes and references

1 J. A. Patterson, *US Pat.*, US3239459A, 1966.
2 A. Bajpayee, *et al.*, *Energy Environ. Sci.*, 2011, **4**, 1672.
3 C. Boo, *et al.*, *Environ. Sci. Technol. Lett.*, 2019, **6**, 359.
4 R. R. Davison, *et al.*, *J. Chem. Eng. Data*, 1966, **11**, 304.
5 L. Lazare, *Desalination*, 1992, **85**, 345.
6 J. S. McNally, *et al.*, *RSC Adv.*, 2020, **10**, 29516.
7 J. Guo, *et al.*, *Nat. Commun.*, 2021, **12**, 437.
8 C. Boo, *et al.*, *ACS EST Eng.*, 2021, **1**, 1351.
9 R. R. Davison, *et al.*, *Desalination*, 1967, **3**, 17.
10 J. R. Vanderveen, *et al.*, *RSC Adv.*, 2018, **8**, 27318.
11 Z. H. Foo, *et al.*, *Trends Chem.*, 2022, **4**, 1078.
12 I. H. Billinge, *et al.*, *Matter*, 2025, **8**, 101879.
13 M. Goral, *et al.*, *J. Phys. Chem. Ref. Data*, 2012, **41**, 043107.
14 M. Goral, *et al.*, *J. Phys. Chem. Ref. Data*, 2012, **41**, 043106.
15 A. D. Wilson and F. F. Stewart, *RSC Adv.*, 2014, **4**, 11039.
16 J. S. McNally, *et al.*, *J. Phys. Chem. B*, 2015, **119**, 6766.
17 R. T. Berry, *et al.*, *ACS Sustainable Chem. Eng.*, 2022, **10**, 3726.
18 P. G. Jessop, *et al.*, *Green Chem.*, 2012, **14**, 1245.
19 A. A. Maryott and E. R. Smith, *Table of Dielectric Constants of Pure Liquids*, U.S. Government Printing Office, 1951.
20 J. C. R. Reis, *et al.*, *Phys. Chem. Chem. Phys.*, 2009, **11**, 3977.
21 R. J. Sengwa and V. Khatri, *Thermochim. Acta*, 2010, **506**, 47.
22 T. Ghorbanpour, *et al.*, *J. Mol. Liq.*, 2018, **260**, 403.
23 M. Reta, *et al.*, *J. Solut. Chem.*, 2001, **30**, 237.
24 F. Pasham, *et al.*, *J. Chem. Eng. Data*, 2020, **65**, 5458.
25 A. Duereh, *et al.*, *J. Phys. Chem. B*, 2016, **120**, 4467.
26 K. M. Shah, PhD thesis, Columbia University, 2024.